A Model-Free Predictive Controller for Networked Microgrids with Random Communication Delays

Sahoo, Subham; Blaabjerg, Frede

Published in:
2021 IEEE Applied Power Electronics Conference and Exposition (APEC)

DOI (link to publication from Publisher):
10.1109/APEC42165.2021.9487438

Publication date:
2021

Document Version
Early version, also known as pre-print

Citation for published version (APA):
Sahoo, S., & Blaabjerg, F. (2021). A Model-Free Predictive Controller for Networked Microgrids with Random Communication Delays. In *2021 IEEE Applied Power Electronics Conference and Exposition (APEC)* (pp. 2667-2672). IEEE (Institute of Electrical and Electronics Engineers). https://doi.org/10.1109/APEC42165.2021.9487438

A Model-Free Predictive Controller for Networked Microgrids with Random Communication Delays

Subham Sahoo and Frede Blaabjerg
Department of Energy Technology
Aalborg University
9220 Aalborg, Denmark
e-mail: {sssa, fbl}@et.aau.dk

***Abstract*—This paper introduces a model-free predictive controller (M-fPC) to allow delay compensation carried out locally in networked microgrids. As the prediction horizon of the existing model predictive controllers (MPC) is limited by communication delays, the proposed controller offers a robust performance and accurate prediction even under large random delayed measurements. Its design philosophy is leveraged by constructing a prediction policy using the inner control loop dynamics in DC networked microgrids. By doing so, the said policy is able to administer the equivalent delay and construct a delay compensation signal accordingly. Finally, its robustness under various communication delay has been simulated under many disturbances and validated experimentally.**

***Index Terms*—Networked microgrids, communication delay, delay compensation**

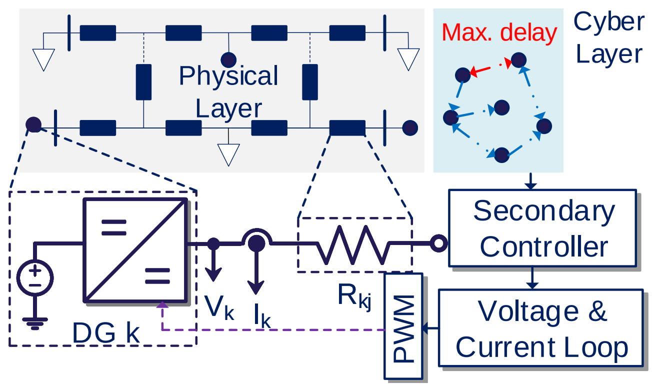

Fig. 1. Networked DC microgrid with N DGs operating with a distributed cyber graph – a cooperative secondary controller is equipped to regulate average voltages and current sharing using local and communicated measurements.

I. Introduction

Over the last few decades, distributed generation (DG) technologies have been used to integrate photovoltaic, wind, and other renewable energy sources into the grid. To quickly harness the value and benefit of DGs, networked microgrids (NMGs) have notably emerged to enhance the flexibility in operation of the modern power grid [1]. As much as they exploit hierarchical control philosophy to facilitate coordination between sources, their coordination is largely affected by specific issues in the cyber layer, such as communication delay, link failure and data packet loss [2]. In particular, these delays may vary in the range of milliseconds to even few seconds, which deteriorates the performance of NMGs. The multiple time-scale property of the hierarchical control causes communication delays among devices, or between equipment and upper control level [3]. These issues arise due to multiple factors such as cyber sampling rate, data volume, cyber topology, data traffic, etc., which ultimately makes it a random parameter in NMGs.

To handle this issue, fixed communication delays are compensated via many ways such as, the weighted average predictive control [8], the gain scheduling [9] and synchronization schemes using multi-timer model [10]. For random communication delays, many delay compensation techniques have been proposed such as generalized predictive control (GPC) [7], networked predictive control (NPC) [8], model predictive control (MPC) [9], Smith predictor [10], delay-dependent observers [11], etc. However, these strategies provide a limited prediction horizon capability. This simply means that the prediction capabilities of these strategies would fail if the maximum communication delay exceeds the defined value.

To address this gap, this paper proposes a model-free predictive controller (M-fPC) for the first time to withstand large random communication delays in NMGs. As the name suggests, it doesn't require any model information yet providing a considerably large prediction horizon to handle random communication delays. The delay compensation is administered by prediction policy, which down samples the error signal that aligns properly with the missing information. Its robustness has been simulated under large communication delay and later validated under experimental conditions.

The rest of the paper is organized as follows. Section II depicts a brief overview of the cyber-physical architecture of DC networked microgrids alongwith a basic overhaul of distributed secondary control objectives and time-delay model and its impact on system operation. Next, the proposed model-free prediction strategy is explained in Section III. Simulations along with experimental validation are presented in Section IV and V, respectively. Finally, Section VI provides the concluding remarks and future scope of this work.

II. Cyber-Physical DC Networked Microgrid

A. Network Preliminaries

As explained above, we consider an example of networked DC MG (shown in Fig. 1) with N DGs communicating to each other using a cooperative cyber graph. Each DG comprises of a DC/DC converter connected directly to a DC source (e.g., renewable energy or energy storage systems). All the DGs are interconnected to each other via tie-line with resistances R_{kj} (shown in Fig. 1) to achieve average voltage restoration and proportionate current sharing. Each unit, represented as an *agent* in the cyber layer, sends and receives $\mathbf{x}_j = [\bar{V}_j, r_j I_j^{pu}]$ from the neighboring agent(s), where the average voltage of j^{th} agent can be given by:

$$\bar{V}_k = V_k + \int_0^{\tau} \sum_{j \in M_k} a_{kj}(\bar{V}_j - \bar{V}_k) d\tau \tag{1}$$

with V_k denoting the measured output voltage of k^{th} agent. Here, $\bar{V}_j$, r_j and I_j^{pu} denote the average voltage estimate, sharing proportionationality constant and per-unit output current of the neighboring agents, respectively. In the cyber layer, each communication digraph is represented via edges to constitute an adjacency matrix $\mathbf{A} = [a_{kj}] \in \mathbf{R}^{N \times N}$, where the communication weights are given by: $a_{kj} = 1, \text{if } (\psi_k, \psi_j) \in \mathbf{E}$, where $\mathbf{E} \subset N \times N$ is a set of all edges connecting two nodes, with ψ_k and ψ_j being the local and neighboring node, respectively. Otherwise, $a_{kj} = 0$. $M_k = \{j \mid (\psi_k, \psi_j) \in \mathbf{E}\}$ denotes the set of all neighbors of k^{th} agent. Further, the in-degree matrix $\mathbf{Z}_{in}$ = diag$\{z_{in}\}$ is a diagonal matrix with its elements, given by $z_{in} = \sum_{k \in M_k} a_{kj}$. Further, the Laplacian matrix $\mathbf{L}$ is defined as $\mathbf{L} = \mathbf{Z}_{in} - \mathbf{A}$. Using these preliminaries, the local control input of the cooperative secondary controller in the presence of maximum communication delay τ_d can be written as:

$$\mathbf{u}_k(t) = \xi_k \sum_{j \in M_k} \underbrace{a_{kj}(\mathbf{x}_j(t - \tau_d) - \mathbf{x}_k(t))}_{\mathbf{e}_{kj}(t)} \tag{2}$$

where $\mathbf{u}_k = [u_k^V, u_k^I]$, $\mathbf{e}_{kj} = [e_{kj}^V, e_{kj}^I]$ respectively as per the elements in x, ξ_k is the convergence variable. Using the Leibnitz formula, we obtain $x(t-\tau_d) = x(t) - \int_{t-\tau_d}^{t} \dot{x}(s)ds$, which can be substituted into (2) in vector representation to get:

$$\dot{\mathbf{x}}(t) = -\mathbf{L}\mathbf{x}(t) - \mathbf{A} \int_{t-\tau_d}^{t} \dot{\mathbf{x}}(s)ds \tag{3}$$

Considering a fixed, undirected and connected cyber graph, all agents will reach equilibrium, if and only if:

$$0 < \tau_d \leq \frac{\pi}{2\sigma_{max}(\mathbf{L})} \tag{4}$$

where σ_{max} is the largest eigenvalue of $\mathbf{L}$. Hence if the communication delay is not bounded inside the limits in (4), $\dot{\mathbf{x}}(t) \neq 0$.

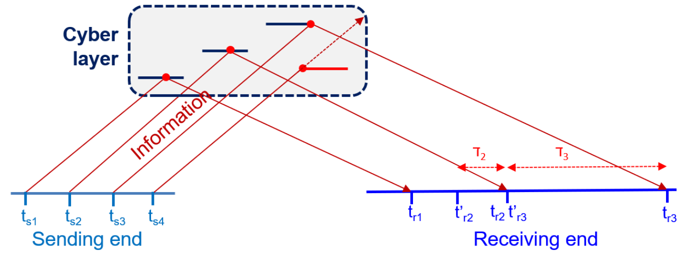

Fig. 2. Information incidence graph implying the reason behind *randomness* in communication delay – cyber layer acts as a stochastic reflecting surface due to traffic in the communication channel.

Using (2), the secondary controller provides control inputs to achieve average voltage regulation and current sharing in the form of voltage correction terms:

$$\Delta V_1^k(t) = H_1(s)(V_{ref} - \bar{V}_k(t)), \Delta V_2^k(t) = -H_2(s)u_k^I(t) \tag{5}$$

where, $H_1(s)$ and $H_2(s)$ are PI controllers. Moreover, V_{ref} is the global reference voltage for all the agents. Finally, the voltage correction terms obtained in (5) are added to V_{ref} to attain the following control objectives:

$$\lim_{t \to \infty} \bar{V}_k(t) = V_{ref}, \lim_{t \to \infty} u_k^I(t) = 0 \ \forall \ k \ \in \ N \tag{6}$$

B. Time Delay System Model

The dynamic model of multiple converters in a DC networked microgrid can be given by:

$$\begin{cases} \dfrac{\mathrm{d}\mathbf{x}_v}{\mathrm{d}t} = -\mathbf{M}\mathbf{I} - \mathbf{V} + \mathbf{u}_V \\ \dfrac{\mathrm{d}\mathbf{x}_i}{\mathrm{d}t} = \mathbf{K}_{V_p}\dot{\mathbf{x}}_v + \mathbf{K}_{V_i}\mathbf{x}_v\mathbf{I} \\ \dfrac{\mathrm{d}\mathbf{I}_c}{\mathrm{d}t} = -\mathbf{L}_g^{-1}(\mathbf{E} - \mathbf{D})\mathbf{V} + \mathbf{L}_g^{-1}\mathbf{V}(\mathbf{K}_{I_p}\dot{\mathbf{x}}_i + \mathbf{K}_{I_i}\mathbf{x}_i) \\ \dfrac{\mathrm{d}\mathbf{V}}{\mathrm{d}t} = -\mathbf{C}^{-1}(\mathbf{E} - \mathbf{D})\mathbf{I}_c + \mathbf{C}^{-1}\mathbf{I}_c(\mathbf{K}_{I_p}\dot{\mathbf{x}}_i + \mathbf{K}_{I_i}\mathbf{x}_i) - \mathbf{C}^{-1}\mathbf{I} \end{cases} \tag{7}$$

where $\mathbf{I} = [I_1, I_2,..., I_N]^T$ is the output current of k^{th} DG, $\mathbf{L}_g$ = *diag*(L_{g_1}, L_{g_2},..., L_{g_N}); L_{g_k} is the converter inductance, $\mathbf{C}$ = *diag*(C_1, C_2,..., C_N); C_k is the output capacitance, $\mathbf{D}$=*diag*(D_1, D_2,..., D_N); D_k represent the duty ratio of k^{th} DG, $\mathbf{I}_c$=*diag*(I_{c_1}, I_{c_2},..., I_{c_N}); I_{c_N} represent the capacitor current of k^{th} DG, $\mathbf{E}$ is the unit matrix, $\mathbf{M}$ = *diag*(M_1, M_2,..., M_k), $\mathbf{u}_V = [u_1, u_2,..., u_k]^T$, $\mathbf{K}_{V_p}$ = *diag*($K_{V_{p1}}$, $K_{V_{p2}}$,..., $K_{V_{pk}}$), $\mathbf{K}_{V_i}$ = *diag*($K_{V_{i1}}$, $K_{V_{i2}}$,..., $K_{V_{ik}}$), $\mathbf{K}_{I_p}$ = *diag*($K_{I_{p1}}$, $K_{I_{p2}}$,..., $K_{I_{pk}}$), $\mathbf{K}_{I_i}$ = *diag*($K_{I_{i1}}$, $K_{I_{i2}}$,..., $K_{I_{ik}}$) are the proportional and integral coefficients of the PI controller in voltage and current control layer, respectively.

Incorporating the cooperative secondary controller in (5) in (7), the time-delay model cn be given by:

$$\dot{\mathbf{x}}(t) - \mathbf{C}_d(t - \tau) = \mathbf{A}_{d0}\mathbf{x} + \mathbf{A}_{d1}\mathbf{x}(t - \tau) \tag{8}$$

where, $\mathbf{A}_{d0}$ = $(\mathbf{I} - \mathbf{A}\mathbf{K}_p)^{-1}\mathbf{K}_i$, $\mathbf{A}_{d1}$ = $(\mathbf{I} - \mathbf{A}\mathbf{K}_p)^{-1}\mathbf{A}_{d0}\mathbf{K}_i$.

Using LMI stability criteria, the maximum delay for which the system remains asymptotically stable can be found out. For different communication graphs, the maximum communication delay will vary.

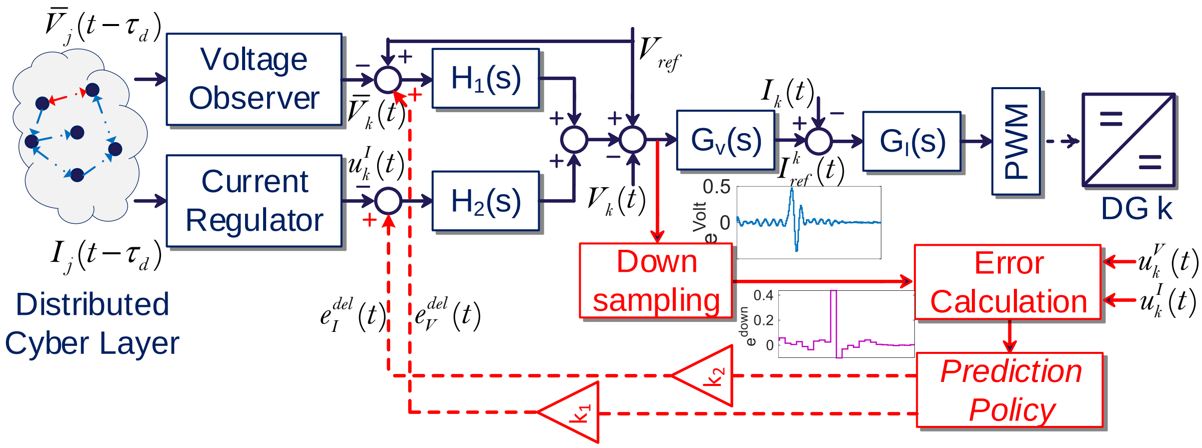

Fig. 3. Proposed model-free predictive controller to handle random communication delays in networked DC microgrid, where $G_V(s)$ and $G_I(s)$ are PI controllers for voltage and current control loops, respectively.

TABLE I
SIMULATION RESULTS OF DIFFERENT TRANSMISSION MEDIUM IN OPNET [2].

Transmission Medium	Maximum latency	Bit error rate
Wired (Narrowband DS0)	0.342 sec	0.02 bit/sec
Wired (Broadband DS3)	0.00053 sec	0 bit/sec
WLAN (IEEE 802.11b/g)	0.029 sec	0.01 bit/sec
GPRS	1.351 sec	0.03 bit/sec

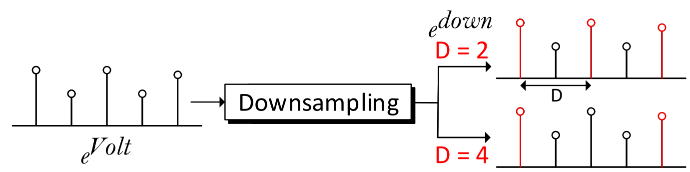

Fig. 4. Downsampling of e^{Volt} into a decimated output e^{down} – Higher the value of the scaling factor D, its resolution keeps decreasing.

To simplify the reason behind variable random delay introduced in the communication channels, an information incidence graph has been used in Fig. 4. It can be seen that two ends have been projected where the sending end broadcasts information and the receiving end receives the information reflected from the reflecting surface, modeled as the cyber layer. The main attribute behind random communication delays is that the cyber layer acts as a stochastic reflecting surface. Considering periodic communication sampled at a given frequency, the information is broadcasted periodically from the sending end, where t_{s2}-t_{s1} = t_{s3}-t_{s2}. As the information lines are reflected *aperiodically* by uneven reflecting surface, it causes random delays. This unevenness in the reflecting surface is a result of many communication factors, such as data packet priority, communication traffic (varying network load), communication medium, number of active servers and operational bandwidth. As a result, in the receiving end, two random delays τ_2 and τ_3 have been encountered, where $\tau_2 \neq \tau_3$. Usually due to the unavailability of server owing to heavy traffic, some information is not reflected back and is often accounted as *missing* information. Hence, this mandates the design of a new strategy which propels an extension of prediction horizon, which is limited in model based delay synchronization schemes [8]-[10]. Although these schemes provide adaptive behavior and low requirement on model precision, they are often limited by their degree of prediction. Additionally, because of detailed model requirements and large computational burden, the practical implementation of such networked prediction schemes are often challenged. To address these points, a model-free predictive controller (M-fPC) is designed for the first time to handle random communication delays in networked microgrids using a novel *prediction policy* using error dynamics of the voltage control layer. More details on its design and modeling has been explained in the next section.

III. Proposed Model-Free Predictive Controller

As shown in Fig. 3, the delayed measurements $x(t - \tau_d)$ mandate prediction of their position in the future. Since the timescale of operation of the secondary controller is generally in seconds, a delay exceeding the pre-defined limits in this range will lead to oscillatory instability due to continually missed updates. This hypothesis has been documented already in Table I using OPNET [13] with different transmission medium, including wired, wireless local area network (WLAN) and GPRS, with TCP/IP as the transmission protocol. It is worth notifying that the results obtained in Table I has been conducted for a ring cyber topology. More details regarding the modeling of the communication layer in OPNET can be obtained from [3]. Previously in [2], it has already been documented that the cooperative secondary controller could establish stable performance only under a delay of 0.342 sec in the wired narrowband DS0 medium. Hence, any random delay beyond this value will make the system unstable.

As MPC usually lays a lot of restrictions on the relationship between the control and the prediction horizon with model-intensive sensitivity on top, its performance has not been substantiated in the presence of large delays yet. It has been shown in Table I that communication delays for different medium can even be in the range of seconds, which is way higher than the control horizon. To minimize dependence on these factors, this paper firstly exploits the PI consensusability law [12] to predicate the response of each control loop in the presence of a disturbance. As the delay compensation takes place in the secondary layer, the error signal $e_k^{Volt}(t)$ prior to the voltage control loop is firstly downsampled to $e_k^{down}(t)$ (as shown in Fig. 3) using:

$$e_k^{down} = \sum_{b=0}^{B-1} e_k^{Volt}[nD - b].h[b] \tag{9}$$

where $h[b]$ is an impulse response with B as the window length and D being the downsampling factor. It is worth notifying that downsampling is a common resampling tool, which decimates the input signal by D sample to reduce the resolution. It is often carried out to decrease the memory requirements. In this context, it is carried out to match the dynamic performance of the error quantity prior to the voltage control loop e_k^{Volt} and the error prior to the secondary controller u_k. This step is mandated to synchronize the abovementioned signals due to the multi-time scale property. A pictorial description of the downsampling operation is provided in Fig. 4, where e^{Volt} is downsampled into two output signals, where the new resolution is scaled by two values of D, i.e, 2 and 4.

To affirm the presence of large and random delays, the downsampled signal $e_k^{down}(t)$ is compared with the local cooperative inputs $u_k^V(t)$ and $u_k^I(t)$ in the local instant. After this stage, the *prediction policy* operates to reconstruct the final delay compensation signals in $\mathbf{e}_k(t_k) = \{e_k^V(t_k), e_k^I(t_k)\}$ locally based on the condition:

$$\mathbf{e}_k(t_k) = e_k^{down}.[1\ 1] - \mathbf{u}_k \tag{10}$$

Finally, this error is then fed into the *prediction policy* stage; which reconstructs another signal to compensate for large delays. Hence, the prediction policy condition can be given by:

$$||\mathbf{e}_k(t_k)|| > \alpha||\text{exp}(-t/T)e_k^{Volt}.[1\ 1]|| \tag{11}$$

where α is a tunable parameter and $T(= K_p/K_i)$ is the controller time constant of $H_1(s)$ and $H_2(s)$ PI control loop. Finally, if the condition in (11) is satisfied, then it generates triggers. These triggers are then used to reconstruct $\mathbf{e}_k(t_k)$ using a `Sample and Hold` block with t_k as the triggering instant. Finally, the reconstructed signals $e_k^V(t_k)$ and $e_k^I(t_k)$, acting as the delay compensating signals, are fed back into the secondary voltage and control loops via tunable gains k_1 and k_2, respectively. These model-free predicted inputs are given by:

$$e_V^{del}(t_k) = k_1 e_k(t_k) \tag{12}$$

$$e_I^{del}(t_k) = k_2 e_k(t_k) \tag{13}$$

Finally as shown in Fig. 3, these inputs are added back into the control inputs of the secondary controller using:

$$u_k^{Vf}(t) = u_k^V(t) + e_V^{del}(t_k) \tag{14}$$

$$u_k^{If}(t) = u_k^I(t) + e_I^{del}(t_k) \tag{15}$$

where, u_k^{Vf} and u_k^{If} are the final secondary control inputs with the model-free predictive inputs in Fig. 3. The efficacy to handle large delays can be accounted specifically to the prediction policy; where the error calculation stage validates an interruption in updated information. As a result, the prediction horizon of MfPC as compared to the existing approaches is much larger.

IV. Simulation Results

The proposed model-free predictive control strategy is tested on cyber-physical DC microgrid, as shown in Fig. 1 with N= 4 DGs for a global reference of 315 V. Each agent of equal power capacities comprising of a DC source and DC/DC buck converter, operate to maintain an output voltage for a local reference $V_{dc_{ref}}^i$ at their respective buses. Its performance is tested for a delay of τ = 1.25 sec alongwith 50% data packet loss. In the first scenario, the M-fPC is arranged with the lowest resolution of D = 5000 for every 50000 samples/sec. However in the second scenario, the downsampling scaling factor is increased to 25000 for every 50000 samples/sec. The simulated plant and control parameters are provided in Appendix.

In Scenario I, the performance of the proposed model-free predictive control strategy is tested for the abovementioned system under a communication delay of 1.25 sec + 50% data packet loss. The proposed control strategy is configured as per D = 5000 for every 50000 samples/sec. Under these circumstances, it can be seen in Fig. 5 that despite large communication delays, the steady-state point is successfully reached. Although the low resolution predicted update $e_{V_1}^{del}$ ensures steady-state convergence, it also leads to elongated settling time of around 0.5 sec. Moreover, it can also be seen that the proposed model-free predictive controller does not interfere with normal operation under physical disturbances, such as load change.

In Scenario II, the performance of the proposed model-free predictive control strategy is tested for the abovementioned system under a communication delay of 1.25 sec + 50% data packet loss and plug and play of DG 2. The proposed control strategy is configured as per D = 25000 for every 50000 samples/sec. Since a higher resolution signal is used, the settling time is faster in Fig. 6 as compared to Scenario I, even though one of the DGs is plugged out and back into the microgrid.

V. Experimental Results

The proposed detection strategy has also been experimentally validated in a DC microgrid with N = 2 DGs ($r_1 = r_2$), as shown in Fig. 7. The validation is carried out using two DC/DC buck converters tied together to a common point of bus comprising a programmable load. Each converter, tied

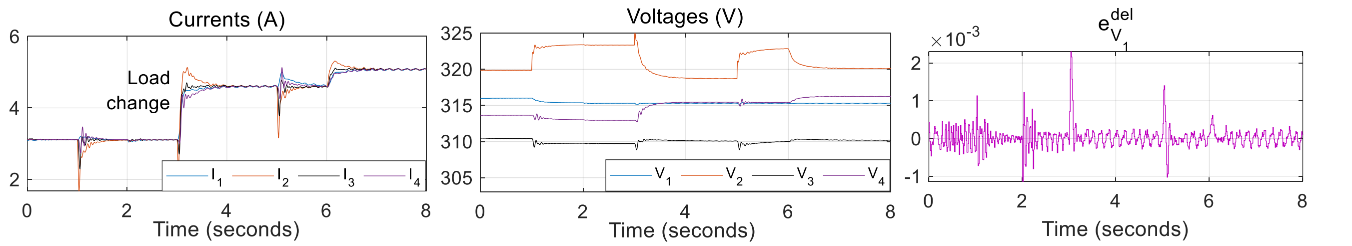

Fig. 5. Performance of the proposed M-fPC under a communication delay of 1.25 sec + 50% data packet loss for a scaling factor D = 5000 for every 50000 samples/sec – the settling time is longer (0.5 sec) although steady-state value is reached.

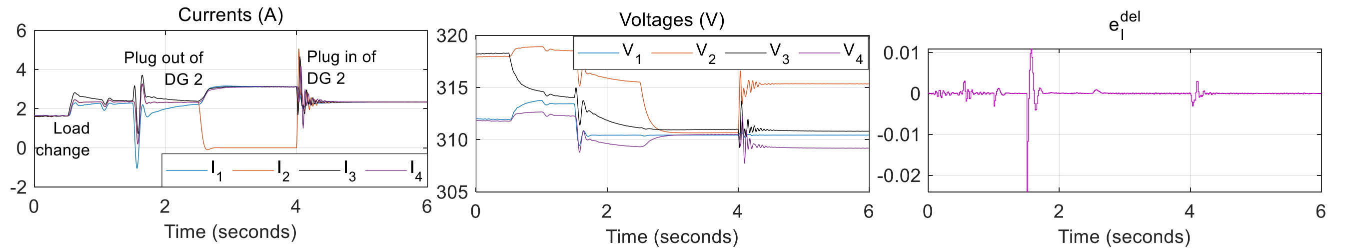

Fig. 6. Performance of the proposed M-fPC under a communication delay of 1.25 sec + 50% data packet loss for a scaling factor D = 25000 for every 50000 samples/sec – the settling time is shorter (0.2 sec) owing to a high resolution signal in comparison with Scenario I.

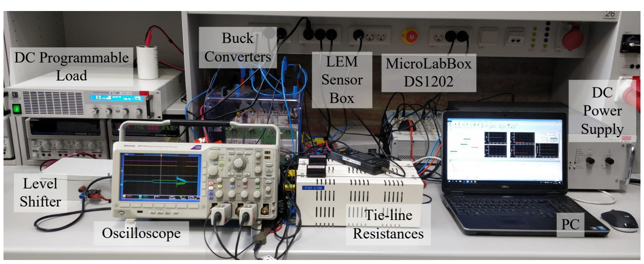

Fig. 7. Experimental setup comprising (a) two commercial DC/DC converters operated in two separated control units to maintain output voltage using distributed cyber network between them to supply power to the (b) programmable DC load.

to a DC source in the input, operates to maintain output voltage across their respective buses. The reference voltage for each converter can be varied in their respective control units, as shown in Fig. 7. Each analog measurement from each converter is communicated to their neighboring control units using USB accompanying the *Modbus* protocol to execute undirected distributed communication. The experimental testbed parameters have been provided in Appendix.

In Fig. 8(a), when a communication delay of 1.75 sec is introduced, the steady-state convergence is disregarded. Further in Fig. 8(b), when a maximum communication delay of (1.15 sec + 75% data packet loss) is introduced, the system goes into oscillatory instability following a load change due to its limited prediction horizon. A communication delay in the range of seconds can typically be observed in GPRS [2]. However, due to the proposed robust *prediction policy*, the performance in attaining (6) is significantly improved for different communication delays upto 1.75 sec and 1.15 sec in Fig. 9(a) and (b), respectively. This improvement can

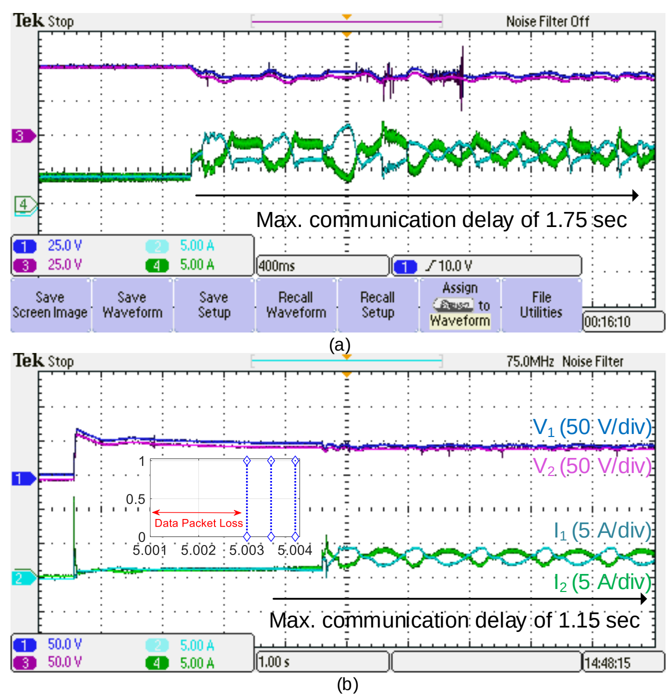

Fig. 8. Limited prediction horizon by MPC [9] leading to oscillatory instability in DC microgrid with N = 2 agents for a communication delay of: (a) 1.75 sec, and (b) 1.15 sec.

be attributed to the reconstructed signals $e^V(t_k)$ and $e^I(t_k)$ (highlighted in Fig. 9) for every disturbance. As soon as the error calculation formalizes that a large delay is prohibiting the next update of measurements, the reconstructed signals using the proposed M-fPC restore consensus between each signal.

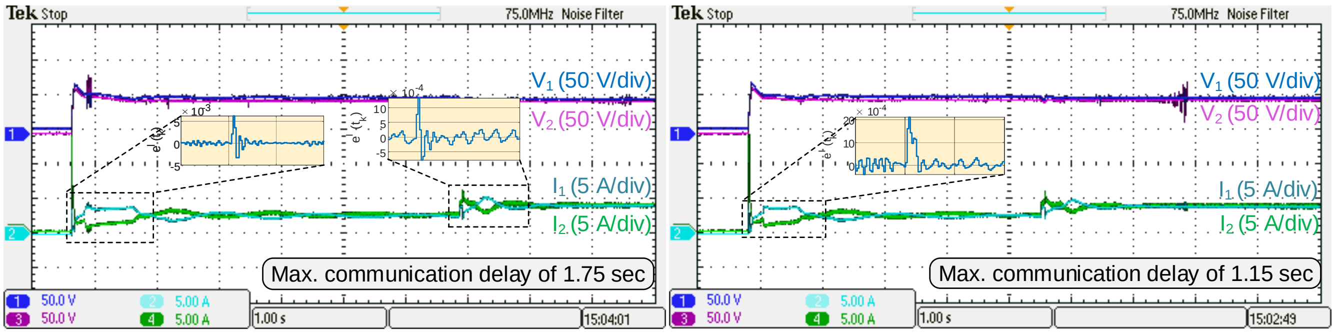

(a) (b)

Fig. 9. Performance of the proposed M-fPC under a communication delay of: (a) 1.75 sec, (b) 1.15 sec.

VI. Conclusion

This paper proposes a model-free predictive controller for the first time to handle random communication delays in networked MG by exploiting the consensusability law and formidably reconstructing a compensating signal locally. In contrast to the existing controllers, M-fPC offers full relaxation to the model-intensive requirements and its corresponding relationship with the prediction accuracy. Its performance is vaidated experimentally for large delays. The future scope of this work will analyze the scalability and investigate the system stability in presence of M-fPC. Furthermore, its working principle and feasibility will be examined in a larger AC and DC networked microgrid.

Appendix

Simulation Parameters

The considered system consists of four sources rated equally for 6 kW. It is to be noted that the line parameter R_{ij} is connected from i^{th} agent to j^{th} agent. Moreover, the controller gains are identical for each agent.

Plant: R_{12} = 1.8 Ω, R_{14} = 1.3 Ω, R_{23} = 2.3 Ω, R_{43} = 2.1 Ω
Converter: L_{se_i}= 3 mH, C_{dc_i}= 250 μF, $I_{dc_{min}}$ = 0 A, $I_{dc_{max}}$ = 18 A, $V_{dc_{min}}$ = 270 V, $V_{dc_{max}}$ = 360 V.
Controller: $V_{dc_{ref}}$= 315 V, $I_{dc_{ref}}$ = 0, $K_P^{H_1}$ = 3, $K_I^{H_1}$ = 0.01, $K_P^{H_2}$ = 4.5, $K_I^{H_2}$ = 0.32, G_{VP} = 2.8, G_{VI} = 12.8, G_{CP} = 0.56, G_{CI} = 21.8, V_{in} = 270 V, k_1 = 0.6, k_2 = 0.93, ξ =2.1, α = 0.1, D = 125, B = 10000.

Experimental Testbed Parameters

The considered system consists of two sources with the converters rated equally for 600 W. It should be noted that the controller gains are consistent for each converter.

Plant: DC/DC buck converters: (L_{se_i}= 3 mH, C_{dc_i}= 100 μF), R_1 = 0.8 Ω, R_2 = 1.4 Ω.
Controller: V_{ref}= 48 V, $K_P^{H_1}$ = 1.92, $K_I^{H_1}$ = 15, $K_P^{H_2}$ = 4.5, $K_I^{H_2}$ = 0.08, k_1 = 0.25, k_2 = 0.74, ξ = 1.8, α = 0.1, D = 75, B = 7500.

Acknowledgment

This work was supported by the Reliable Power Electronics-Based Power System (REPEPS) project at the Department of Energy Technology, Aalborg University, as a part of the Villum Investigator Program funded by the VELUX Foundation.

References

[1] Y. Li, P. Zhang, and M. Yue, "Networked microgrid stability through distributed formal analysis," *Applied Energy*, vol. 228, pp. 279-288, 2018.

[2] S. Sahoo and S. Mishra, "A Distributed Finite-Time Secondary Average Voltage Regulation and Current Sharing Controller for DC Microgrids," *IEEE Trans. Smart Grid*, vol. 10, no. 1, pp. 282-292, Jan 2019.

[3] S. Sahoo, et. al., "Investigation of Distributed Cooperative Control for DC Microgrids in Different Communication Medium," *Energy Procedia*, vol. 142, pp. 2218-2223, 2017.

[4] Z. Wu, H. Fang, and Y. She, "Weighted average prediction for improving consensus performance of second-order delayed multi-agent systems," *IEEE Transactions on Systems, Man, and Cybernetics, Part B (Cybernetics)*, vol. 42, no. 5, pp. 1501-1508, Oct. 2012.

[5] H. Fang, Z. Wu, and J. Wei, "Improvement for consensus performance of multi-agent systems based on weighted average prediction," *IEEE Transactions on Automatic Control*, vol. 57, no. 1, pp. 249-254, Jul. 2012.

[6] S. Liu, X. Wang, and P. X. Liu, "Impact of communication delays on secondary frequency control in an islanded microgrid," *IEEE Transactions on Industrial Electronics*, vol. 62, no. 4, pp. 2021-2031, Apr. 2015.

[7] T. Liu, et. al., "Analysis and design of the time-delay compensation for networked control systems with random communication delay," *Proc. 35th Chinese Control Conf.*, pp. 7234-7239, 2016.

[8] G. P. Liu, "Predictive controller design of networked systems with communication delays and data loss," *IEEE Trans. on Circuits and Systems II: Express Briefs*, vol. 57, no. 6, pp. 481-485, Jun. 2010.

[9] T. V. Vu, et al., "Model predictive control for power control in islanded DC microgrids," *IECON 2015-41st Annual Conference of the IEEE Indus. Electron. Society*, pp. 1-5, 2015.

[10] Z. Wang, J. Xu, and H. Zhang, "Consensus seeking for discrete-time multi-agent systems with communication delay," *IEEE/CAA Journal of Automatica Sinica*, vol. 2, no. 2, pp. 151-157, Apr. 2015.

[11] S. Sahoo, S. Mishra, S. Jha, B. Singh, "A Cooperative Adaptive Droop Based Energy Management & Optimal Voltage Regulation Scheme for DC Microgrids," *IEEE Trans. Ind. Electron.*, vol. 67, no. 4, pp. 2894-2904, Apr. 2020.

[12] R. Carli, et. al., "A PI consensus controller for networked clocks synchronization," *IFAC Proceedings*, vol. 41, no. 2, pp. 10289-10294, 2008.

[13] X. Chang, "Network simulations with OPNET." *WSC'99. 1999 Winter Simulation Conference Proceedings.'Simulation-A Bridge to the Future*, vol. 1, pp. 307-314, 1999.